Received: 4 October 2021 Revised: 10 November 2021 Accepted article published: 16 November 2021 Published online in Wiley Online Library: 27 November 2021

(wileyonlinelibrary.com) DOI 10.1002/pi.6327

Self-assembly of block copolymers for biological applications

Zili Li[a,b] and Zhiqun Lin[a*]

Abstract

Self-assembly of block copolymers (BCPs) has garnered much attention over the past several decades owing to an array of intriguing properties. In this perspective, recent advances in self-assembly and applications of BCPs with different architectures are presented. First, the self-assembly mechanism of BCPs and the general criteria to evaluate the assembled morphologies are introduced. Subsequently, the self-assembly of linear, star-like and bottlebrush-like BCPs is discussed. In particular, polymerization-induced self-assembly for large-scale preparation is highlighted. Afterwards, a rich diversity of applications of self-assembled BCPs in drug delivery, bioimaging, molecular recognition and photothermal therapy are outlined. Finally, an outlook on larger-scale production and implementation of self-assembled BCPs for biological applications is noted.

Keywords: self-assembly; star-like block copolymers; bottlebrush-like block copolymers; biological applications

Self-assembly is widely recognized as a unique process of organizing components into organized nanostructures without external intervention. This phenomenon is ubiquitous in biological systems from deoxyribonucleic acid (DNA) with a double helix to lipid bilayer-containing cell membrane. Inspired by such a versatile process, abundant self-assemblies (e.g. spherical, cylindrical and lamellar micelles) have been achieved by capitalizing on rationally designed molecules (e.g. surfactants, block copolymers etc.) via various types of supramolecular interactions, including host–guest, hydrophobic, hydrogen-bonding and electrostatic interactions.[1] Among the molecules of interest, block copolymers (BCPs) have been extensively investigated over the past decades due to their diverse architectures (e.g. linear, star-like, bottlebrush-like etc.) as well as their excellent physical and mechanical properties. Notably, with the development of robust living polymerization techniques (e.g. reversible addition-fragmentation chain transfer polymerization, atom transfer radical polymerization (ATRP), nitroxide-mediated radical polymerization and ring-opening metathesis polymerization), the architectures noted above have been readily accessed. Moreover, a variety of morphologies have been observed in the bulk state or in selective solvents owing to the versatile pathways for preparing hierarchical BCPs and the accessible bottom-up self-assembly process. Additionally, composition-dependent BCPs, such as functional moieties, have been incorporated into the building blocks via highly efficient reactions to explore the composition effect on self-assembly. As such, the self-assembly of BCPs has garnered considerable interest for potential biological applications in drug delivery, bioimaging, molecular recognition and photothermal therapy (Fig. 1).

Despite the ability to organize into diverse morphologies, it is challenging to fully control the self-assembly of BCPs as it depends sensitively on their architectures and compositions as well as the states (e.g. solvents, polarity and pH of the solutions, surface chemistry of solid substrate etc.). Such dependence is dictated by the need to lower the free energy of the constituent blocks in solution (or air), thus achieving the thermodynamic equilibrium of the system. The packing parameter $p = v/al$, where a is the section area per polymer chain and v and l are the volume and length of the hydrophobic tail chain, respectively, has been applied to predict the assembled morphology of BCPs in solution.[2] Although several parameters such as solvent polarity, pH and temperature will affect the self-assembly behavior in solution, the packing parameter can be employed to direct the design and synthesis of BCPs with complex structures. Moreover, great efforts have been centered on pursuing hierarchically ordered architectures by exploiting the stepwise self-assembly of BCPs to mimic sophisticated biomaterials, in which the assembled micelles are used as building blocks for further assembly.[3] Diverse self-assembled morphologies of BCPs have been achieved in both experimental and computational results. Therefore, in the latter context, theoretical simulation has also been extensively applied to reveal the mechanism of self-assembly of BCPs and guide the synthesis of BCPs as well as the selection of assembling conditions.

Linear BCPs represent the most widely studied system for self-assembly. Amphiphilic diblock copolymers self-assemble into different morphologies including spheres, rods, lamellae and vesicles in solution (i.e. a mixture of organic solvent and water) by tuning the solvent polarity at a concentration above the critical micelle concentration. To achieve the minimized free energy,

* Correspondence to: Z Lin. E-mail: zhiqun.lin@mse.gatech.edu

a School of Materials Science and Engineering, Georgia Institute of Technology, Atlanta, GA, USA

b Center of Micro-Nano System, School of Information Science and Technology, Fudan University, Shanghai, China

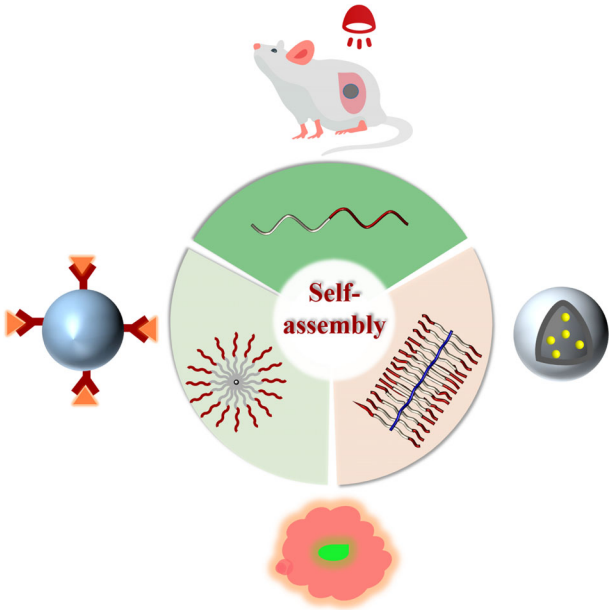

Figure 1. Various architectures of block copolymers, including linear, star-like and bottlebrush-like polymers, and their biomedical applications.

amphiphilic BCPs are usually assembled into spherical micelles with hydrophobic blocks located in the inner compartment and hydrophilic blocks forming the corona towards the solvent (i.e. a 'crew-cut' or 'star-like' micelle, depending on the length of the two blocks). Generally, BCPs first dissolved in the organic solvent; with the introduction of water, they self-assembled into more complicated structures because of the presence of various interactions between different blocks and solvents. In a similar manner to linear BCPs, amphiphilic dendritic-linear BCPs with precisely defined water-soluble peripheral poly(ethylene glycol) (PEG) tails could directly self-assemble into polymer cubosomes in an aqueous solution of dioxane and water. Increasing the water content affects the resulting average diameter and size distribution of assemblies.[4] In addition, single branched-linear block copolymers could assemble from vesicle to inverse mesophases with desired lattices by tuning the cosolvents due to the affinity of the solvent toward the polystyrene (PS) block.[5]

For self-assembly of BCPs in the bulk state, inherent immiscibility of dissimilar blocks induces microphase separation, forming a set of nanostructures (i.e. spheres, cylinders, gyroids and lamellae) that depend on the volume fractions of the two blocks. The size of the phase-separated domains can be tuned from a few to several hundred nanometers by manipulating their compositions and molecular weights. As the domain size d is related to N and χ (i.e. $d \propto N^{2/3}\chi^{1/6}$), where N is the overall degree of polymerization of the BCP and χ is the Flory–Huggins interaction parameter between the blocks, then d can be readily tailored by controlling N and χ. For instance, a hexagonally close-packed sphere phase can be achieved from linear block copolymer with high χ across a wide range of compositions, which is supported by the experimental and simulation results.[6] Beyond χ, complex inaccessible morphologies from linear BCPs can be obtained by manipulating the combination parameters (e.g. local charge density and counterion properties) of the system, which can change the intermolecular interactions and the free energy balance. Charged block copolymers, poly[oligo(ethylene glycol) methyl ether methacrylate-*co*-oligo(ethylene glycol) propyl sodium sulfonate methacrylate]-*block*-polystyrene (POEGMA-*b*-PS), with various chain lengths are self-assembled into an intriguing superlattice lamellar morphology in the melt state (Fig. 2).[7] As the charge density of the BCPs increases, the morphologies transfer from disordered to lamellar structures. Additionally, doping with free salt is also favorable for the formation of superlattice morphology due to the local electrostatic interactions in the POEGMA microdomain phase.[7]

Notably, most BCPs are synthesized using petrochemicals. In contrast, far less researched biocompatible and biodegradable polypeptide-, poly(lactic acid)- and cellulose-based BCPs merit increasing attention for further biomedical applications. Moreover, the typical domain size of self-assembled nanostructures of BCPs in bulk is smaller than 50 nm; self-assembly with a larger domain size and faster assembly kinetics (aiming to avoid possible thermal or solvent treatment) in film for biological separation is rarely explored probably due to the difficulty in synthesizing polymers with ultra-high molecular weight and the resulting high viscosity. Synthesis of BCPs possessing complex structures (e.g. star-like and bottlebrush-like) with fewer chain entanglements could confer the possibility of solving these issues.

Star-like BCPs can be regarded as linear BCPs that are cross-linked with a central core. This unique architecture gives them unique characteristics such as lower solution viscosity due to the fewer arm entanglements.[8] Cyclodextrin is a kind of biocompatible material containing many hydroxyl groups on its periphery, which is favorable for post-modification and functions as an initiator. Cyclodextrin-based star-like BCPs containing amphiphilic linear arms form core–shell globular structures, thereby facilitating the assembly of monodisperse spherical micelles in solution.[9] When functional blocks of interest are introduced to the unimolecular star-like BCPs via living radical polymerization, they demonstrate multiple stimuli-responsive attributes with high sensitivity due to the presence of high-density moieties. A series of amphiphilic star-like poly(4-vinyl pyridine)-*block*-poly(*tert*-butyl acrylate) (P4VP-*b*-P*t*BA) with well-defined molecular architectures are achieved via sequential ATRP. When the P*t*BA block is hydrolyzed into PAA, dual pH-responsive star-like P4VP-*b*-PAA can be readily obtained. With high and low pH values star-like P4VP-*b*-PAA forms uniform micelles due to the solubility of the inner or outer blocks, while in the middle range of pH values (e.g. $5 < \text{pH} < 8$) it yields a large aggregate owing to the electrostatic interaction between PAA and P4VP blocks.[9]

It is noteworthy that the implementation of miktoarm star-like BCPs bearing different arms may provide a straightforward strategy for constructing multicompartment nanoparticles, which could deliver cargos in one micelle with different disassembly behaviors induced by different stimuli. Unlike the extensively studied linear BCP-based micelles for drug delivery, more attention should be directed to understanding the delivery behavior of star-like BCPs.

Bottlebrush-like polymers (BBPs) (including bottlebrush block copolymers, core–shell BBPs where side chains are amphiphilic block copolymers etc.) are an intriguing class of polymers in which the side chains are tethered to each repeating unit of a linear backbone.[10] The densely grafted side chains of BBPs experience significant steric repulsion, resulting in the absence of entanglement even at higher molecular weights. The other appealing characteristic of BBPs is their cylindrical morphology in solution arising from the steric repulsion effect. Such unique conformation

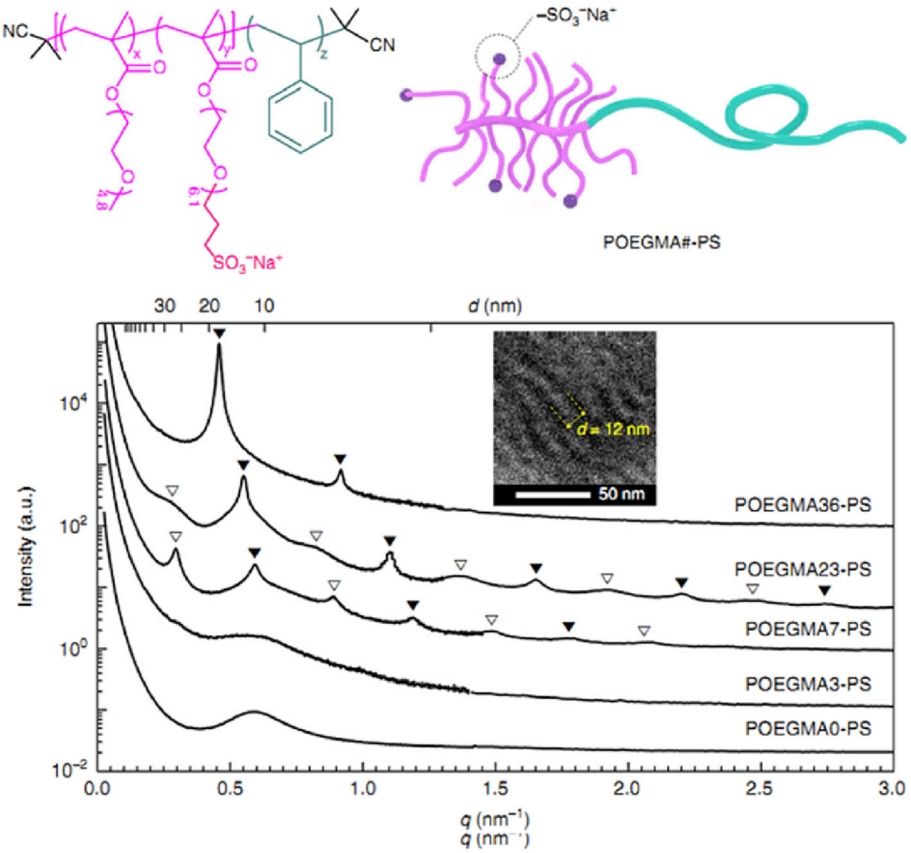

Figure 2. Chemical structure of POEGMA-*b*-PS (upper panel) and small-angle and mid-angle X-ray scattering combined profiles of a series of BCPs at 80 °C (lower panel). Reproduced with permission from reference.[7] Copyright 2019 Nature Publishing Group.

of BBPs is largely determined by the structure parameters (e.g. grafting density, side chain length and backbone length). For instance, when BBPs have comparable side chain length to that of backbone, they form spherical micelles. Increasing the backbone length induces the formation of cylindrical micelles. The diameter and length of the resulting cylindrical micelles are governed by the intrinsic side chain and backbone lengths of BBPs, respectively. Diverse hierarchically assembled architectures have been made via the self-assembly of BBPs in selective solvents. Similar to linear triblock copolymers, triblock bottlebrush copolymers can also self-assemble into micelles and networks under different conditions. "ABC" bottlebrush triblock copolymers bearing an inner poly(lactic acid) (PLA) block, an intermediate PEG block and an outer poly(*N*-isopropylacrylamide) (PNIPAM) block assemble into uniform ~100 nm micelles in an aqueous solution, in which the PLA blocks and PNIPAM are located in the core and outside, respectively.[11] The size of micelles from BBPs is much larger than that of micelles assembled from linear BCPs, thereby increasing the encapsulation amount of therapeutic agents. Heating the micellar solutions of triblock bottlebrush copolymers over the lower critical solution temperature of PNIPAM, the PLA and PNIPAM domains will serve as physical crosslinkers, inducing the formation of a network with large pore size and sustained release of drugs.[11] This strategy significantly improves both the efficacy and safety of cancer immunotherapies.

More importantly, self-assembled morphologies with a much larger domain size (>100 nm) can be conveniently accessed because of the ultra-high molecular weight and lack of entanglement of BBPs. Additionally, the diverse side chains in bottlebrush block copolymers and core–shell BBPs could also afford more compartments or functional sites for biomedical applications (e.g. drug delivery, bioimaging and molecular recognition). For example, polysaccharide-based BBPs bearing amphiphilic diblock copolymers are synthesized via ATRP. The amphiphilicity induces the self-assembly of micelles with the drug encapsulated in the inner core, which can be released in acid conditions.[12] Therefore, this class of BCPs also opens up a new avenue to explore shape-dependent drug delivery behavior.

It is worth noting that the self-assembly of BCPs via multiple steps in dilute solution (i.e. low yields) could greatly limit their large-scale production and implementation. In this context, the emerging polymerization-induced self-assembly (PISA) could offer a potential solution to overcome this limitation, in which self-assembly proceeds during dispersion polymerization or emulsion polymerization. With the chain extension of hydrophilic macroinitiator via advanced polymerization techniques, the amphiphilic BCPs experience ergodic morphology transitions (e.g. from spheres to worms or nanotubes) during the polymerization process as a result of the systemic variation of the packing parameter.[13] For instance, self-assembly of linear and star-like block copolymers, [poly(4-vinyl pyridine)-*block*-polystyrene]$_n$ ([P4VP-*b*-PS]$_n$), with various arms prepared via PISA has been systematically explored.[14] This architectural effect on the assemblies is clearly correlated to the arm numbers. With the increase in arms, the vesicle size of star-like BCP is much larger than that of linear BCP because of the stretched PS chains derived from the increased steric repulsion of the P4VP arms.[14] In particular, the PISA process can also be performed under mild

conditions, which is favorable for *in situ* encapsulation of therapeutic agents or drugs with high yield.

The dynamic nature in conjunction with cavities that emerged from self-assembled micelles renders them promising candidates for drug delivery. External stimuli-responsive moieties (e.g. pH-sensitive) can be easily introduced to BCPs because of the intriguing structure controllability, thus resulting in superior *in vitro* and/or *in vivo* activities.[2] BBPs with hydrophilic polysaccharide as the backbone and amphiphilic diblock copolymers (hydrophobic anticancer drug doxorubicin (DOX) is tethered in the outer block with hydrazine bonds) as side chain are assembled into micelles (denoted as DOM@DOX), in which the hydrophilic backbone and the side chain act as steric shielding for the inner DOX-containing blocks owing to the densely grafted side chains (Fig. 3). Moreover, the hydrophilic backbone and the side chain improve the stability in solution and affinity to cells. Therefore, the micelles readily penetrate the cells via an enhanced permeability and retention (EPR) effect. The acid condition in tumor cells induces the destruction of micelles to release DOX from BBPs, demonstrating enhanced intratumoral permeability and significant tumor suppression efficiency.[12]

In addition, shape anisotropy has demonstrated great potential in drug delivery applications. The readily tailored size and shape of self-assembled morphologies are favorable for scrutinizing the effect of shape anisotropy on drug delivery capability. Notably, cylindrical micelles exhibit enhanced association and penetration to cells, thus improving the retention and efficiency of drugs.[15] However, the effect of nanoparticle aspect ratio and topology on polymer micelles is difficult to investigate due to the synthetic challenges in producing uniform nanomaterials with one type of polymer. In this regard, much effort could be devoted to studying BBP-based self-assembly to further understand the underlying mechanism and improve the enhanced efficiency. In addition, the ability to rationally design and synthesize BCPs with different architectures and compositions allows for exploration of the composition effect on shape anisotropy -tuned-drug delivery. As BBPs possess multifunctional side chains, they could carry cargos for drug delivery, moieties for molecular recognition and fluorescent sites for bioimaging.[16] However, cargo loading efficiency still needs to be improved for practical applications. It is interesting to note that aggregation-induced emission is based on molecular aggregation.[17] As such, it can readily be

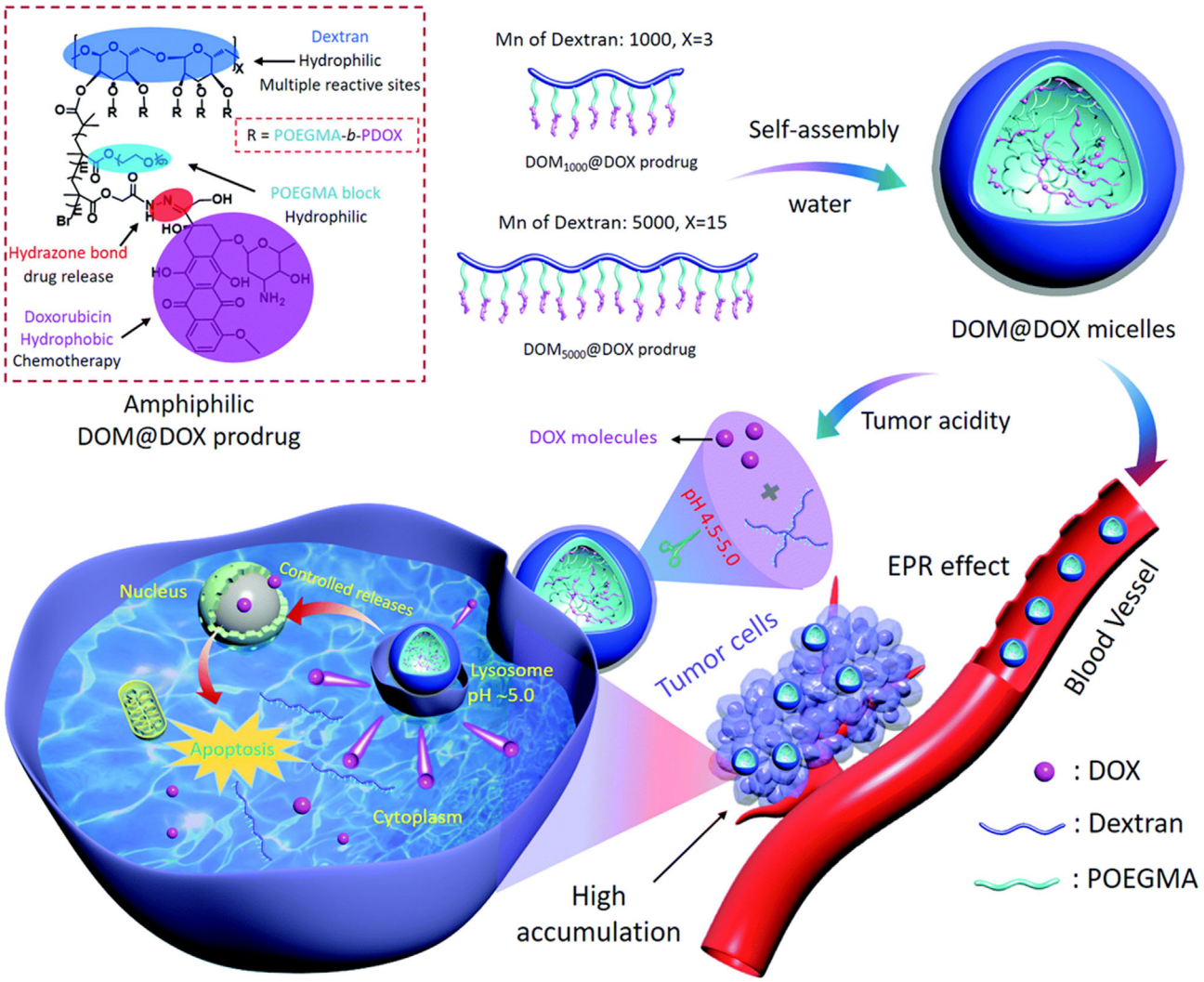

Figure 3. Schematic illustrations of the synthetic route to DOM@DOX micelles, drug accumulation via the EPR effect, cell internalization process, and pH-responsive drug release mechanism. Copyright 2020. Reproduced with permission from the Royal Society of Chemistry.

combined with self-assembly by anchoring fluorophores on BCPs. Consequently, the self-assembly process can be visualized through the color change and the resulting micelles can be applied for bioimaging and drug delivery. Likewise, conjugated polymers have been employed as building blocks for self-assembly, in which near-infrared absorption and fluorescence have been demonstrated for deep-tissue optical imaging and phototherapy.[18] Thus, introducing these conjugated moieties to star-like or bottlebrush-like polymers may enhance the efficiency. Furthermore, the functional moieties of BCPs can coordinate with noble metal nanocrystals (e.g. gold nanorods). The resulting nanocomposites can function as photothermal agents for photothermal therapy.[19] More importantly, self-assembled gold nanorods or nanoparticles further enhance the plasmonic coupling, thereby effectively boosting the therapy efficiency with more bio-friendly near-infrared light.[20]

In summary, the past several decades have witnessed advances in the self-assembly of BCPs and its utility in biomedical applications. The key to the revolution of the self-assembly of BCPs in the future may lie in the ability for their large-scale production and implementation for practical biomedical applications. Nonetheless, with progressive effort on self-assembly of BCPs, this limitation will be overcome.

ACKNOWLEDGEMENTS

This work is supported by the Air Force Office of Scientific Research (FA9550-19-1-0317) and NSF (CMMI 1914713, Chemistry 1903957).

REFERENCES

1 Li Z and Lin Z, *ACS Nano* **15**:3152–3160 (2021).
2 Mai Y and Eisenberg A, *Chem Soc Rev* **41**:5969–5985 (2012).
3 Lu Y, Lin J, Wang L, Zhang L and Cai C, *Chem Rev* **120**:4111–4140 (2020).
4 La Y, Park C, Shin TJ, Joo SH, Kang S and Kim KT, *Nat Chem* **6**:534–541 (2014).
5 La Y, An TH, Shin TJ, Park C and Kim KT, *Angew Chem Int Ed* **54**:10483–10487 (2015).
6 Zhang C, Vigil DL, Sun D, Bates MW, Loman T, Murphy EA *et al.*, *J Am Chem Soc* **143**:14106–14114 (2021).
7 Shim J, Bates FS and Lodge TP, *Nat Commun* **10**:1–7 (2019).
8 Liu Y, Wang J, Zhang M, Li H and Lin Z, *ACS Nano* **14**:12491–12521 (2020).
9 Harn Y-W, He Y, Wang Z, Chen Y, Liang S, Li Z *et al.*, *Macromolecules* **53**:8286–8295 (2020).
10 Li Z, Tang M, Liang S, Zhang M, Biesold GV, He Y *et al.*, *Prog Polym Sci* **116**:101387 (2021).
11 Vohidov F, Milling LE, Chen Q, Zhang W, Bhagchandani S, Nguyen HV-T *et al.*, *Chem Sci* **11**:5974–5986 (2020).
12 Zhang T, Wang Y, Ma X, Hou C, Lv S, Jia D *et al.*, *Biomater Sci* **8**:473–484 (2020).
13 Liu C, Hong C-Y and Pan C-Y, *Polym Chem* **11**:3673–3689 (2020).
14 Zhang Y, Cao M, Han G, Guo T, Ying T and Zhang W, *Macromolecules* **51**:5440–5449 (2018).
15 Müllner M, Yang K, Kaur A and New EJ, *Polym Chem* **9**:3461–3465 (2018).
16 Sowers MA, McCombs JR, Wang Y, Paletta JT, Morton SW, Dreaden EC *et al.*, *Nat Commun* **5**:1–9 (2014).
17 Feng H-T, Lam JW and Tang BZ, *Coord Chem Rev* **406**:213142 (2020).
18 Miao Q and Pu K, *Adv Mater* **30**:1801778 (2018).
19 Du Y, Jiang Q, Beziere N, Song L, Zhang Q, Peng D *et al.*, *Adv Mater* **28**:10000–10007 (2016).
20 Murphy CJ, Chang H-H, Falagan-Lotsch P, Gole MT, Hofmann DM, Hoang KNL *et al.*, *Acc Chem Res* **52**:2124–2135 (2019).

